

CLIPer: Hierarchically Improving Spatial Representation of CLIP for Open-Vocabulary Semantic Segmentation

Lin Sun¹, Jiale Cao¹, Jin Xie², Xiaoheng Jiang³, Yanwei Pang^{1,4}
¹Tianjin University ²Chongqing University ³Zhengzhou University
⁴Shanghai Artificial Intelligence Laboratory
 {sun0806, connor, pyw}@tju.edu.cn
 xiejin@cqu.edu.cn, jiangxiaoheng@zzu.edu.cn

Abstract

Contrastive Language-Image Pre-training (CLIP) exhibits strong zero-shot classification ability on various image-level tasks, leading to the research to adapt CLIP for pixel-level open-vocabulary semantic segmentation without additional training. The key is to improve spatial representation of image-level CLIP, such as replacing self-attention map at last layer with self-self attention map or vision foundation model based attention map. In this paper, we present a novel hierarchical framework, named CLIPer, that hierarchically improves spatial representation of CLIP. The proposed CLIPer includes an early-layer fusion module and a fine-grained compensation module. We observe that, the embeddings and attention maps at early layers can preserve spatial structural information. Inspired by this, we design the early-layer fusion module to generate segmentation map with better spatial coherence. Afterwards, we employ a fine-grained compensation module to compensate the local details using the self-attention maps of diffusion model. We conduct the experiments on seven segmentation datasets. Our proposed CLIPer achieves the state-of-the-art performance on these datasets. For instance, using ViT-L, CLIPer has the mIoU of 69.8% and 43.3% on VOC and COCO Object, outperforming ProxyCLIP by 9.2% and 4.1% respectively. We release the source code and models at <https://linsun449.github.io/cliper>.

1. Introduction

Open-vocabulary semantic segmentation [2, 49, 51] aims to divide an image into different groups and assign each group a label belonging to arbitrary semantic categories. Compared to the traditional semantic segmentation, open-vocabulary semantic segmentation is a more challenging segmentation task. Recently, the researchers mainly explored to employ vision-language models for open-

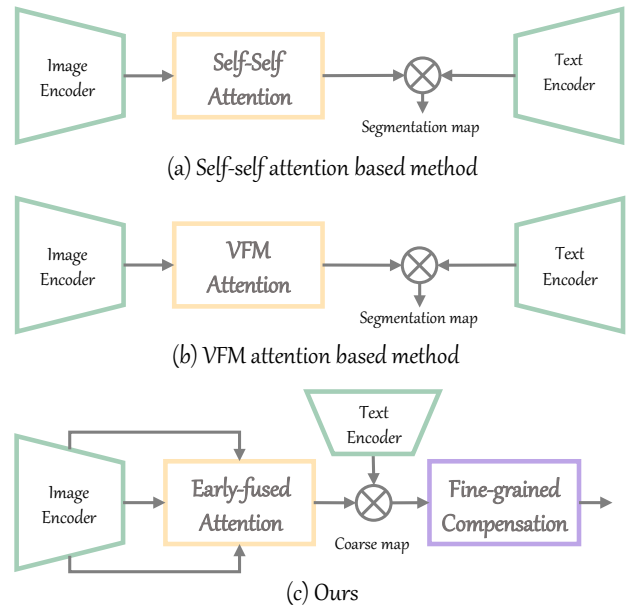


Figure 1. Comparison with existing CLIP-based open-vocabulary semantic segmentation approaches without training. In (a), several approaches [9, 16, 34] replace the original self-attention map at last layer with self-self attention map, which can better maintain spatial coherence. In (b), the method ProxyCLIP [15] opts for a different strategy, replacing original self-attention map with vision foundation model-based (VFM-based) attention map. In (c), we utilize the embeddings and self-attention maps at early layers to fully exploit spatial information within CLIP. Subsequently, we perform fine-grained compensation using diffusion model to further improve local details.

vocabulary semantic segmentation. The related methods can be divided into training-based [8, 47, 48] and training-free [16, 34, 51] approaches. Compared to training-based approaches, training-free counterparts are simpler.

Contrastive Language-Image Pre-training (CLIP) model [25] has shown strong zero-shot capabilities on image-level

classification task, due to the pre-training on large-scale image-text paired data [30]. Based on this, several methods have been proposed to adapt CLIP for training-free open-vocabulary semantic segmentation. The key challenge is to improve spatial representation of image-level supervised model for pixel-level segmentation. As shown in Fig. 1(a), some methods modify the original self-attention map at last layer with self-self attention map, better maintaining local spatial information. For instance, MaskCLIP [51] employs an identical self-self matrix as the self-attention map at last layer to generate visual patch embeddings, while SCLIP [34] and ClearCLIP [16] employ the query-to-query or key-to-key attention map to replace original self-attention map. Instead of using original or self-self attention map, ProxyCLIP [15] extracts the self-attention map from visual foundation model (VFM) [4] as self-attention map at last layer in Fig. 1(b). These methods enhance segmentation performance of CLIP in open-vocabulary setting without additional training. However, these methods mainly consider improving the self-attention map at last layer of CLIP.

In this paper, we focus on two factors to hierarchically improve spatial representation. (i) The first one is to improve patch-level spatial coherence similar to existing methods [9, 16]. We observe that, the patch embeddings and attention maps at early layers contain rich spatial structural information. Therefore, instead of using self-self or VFM-based attention at last layer, we aim to exploit early-layer information of CLIP. (ii) The second is fine-grained compensation. The patch-level similarity map between image and text is relatively coarse in local details. It is necessary to further improve local details for improved segmentation.

Based on these two factors above, we introduce a novel hierarchical method for open-vocabulary semantic segmentation, named CLIPer. Our CLIPer consists of an early-layer fusion module and a fine-grained compensation module. As shown in Fig. 1(c), the early-layer fusion module integrates patch embeddings and attention maps from early layers to improve spatial coherence of output patch embeddings. Based on the output patch embeddings and text embeddings of arbitrary categories, we can generate the coarse segmentation map. Afterwards, the fine-grained compensation module integrates fine spatial information of Stable Diffusion to compensate the local details. We conduct experiments on various segmentation datasets. The contributions and merits are summarized as

- We propose a novel training-free CLIP-based method that hierarchically improves the spatial representation of CLIP for open-vocabulary semantic segmentation.
- An early-layer fusion strategy is introduced to improve patch-level coherence within CLIP by integrating early-layer information.
- A fine-grained compensation module leverages the fine detail information from diffusion model to refine local de-

tails lost in CLIP, leading to more precise segmentation.

- Our method achieves the superior performance on various segmentation datasets. For instance, using ViT-L backbone, it achieves mIoU scores of 69.8% and 43.3% on VOC and Object, respectively.

2. Related Work

Vision-language pre-training models. Vision-language pre-training models aim to establish relationships between the images and texts. Among these models, CLIP [25] is one of most successful vision-language models, which is trained on a very large-scale image-text paired dataset. Due to the large-scale pre-training, CLIP exhibits strong zero-shot classification performance on various image-level tasks. OpenCLIP [7] explores to improve CLIP via conducting a comprehensive experimental analysis of scaling laws. To address the challenge of expensive image-text annotations, ALIGN [12] introduces to use large-scale noisy image-text data for model learning.

Open-vocabulary semantic segmentation. Compared to traditional semantic segmentation [22, 40] sharing a fixed category set between the training and test sets, open-vocabulary semantic segmentation [20, 26, 31] aims to segment the objects belonging to arbitrary categories. In the past years, open-vocabulary semantic segmentation has attracted great attention, and achieved substantial progress. The related methods can be divided into training-based [5, 23, 27, 44] and training-free [21, 34] approaches. Training-based methods first train a model on a fixed set of categories from a given training dataset and then apply the learned model to segment objects from arbitrary semantic categories. Some training-based approaches [19, 45] follow two-stage pipeline, where the first stage extracts the mask proposals, and the second stage assigns semantic labels to mask proposals. For instance, OVSeg [19] first trains a class-agnostic mask proposals using query-based framework Mask2Former [6], and then fine-tunes CLIP to classify the cropped and masked images. Some training-based approaches adopt single-stage pipeline. For instance, SAN [47] introduces a side adapter to adapt CLIP for both classification and segmentation. SED [39] introduces a simple encoder-decoder architecture with category early rejection for fast inference. CAT-Seg [8] constructs pixel-level cost map for segmentation. SAM-CLIP [35] integrates CLIP and SAM [14] into a single multi-task segmentation.

Compared to training-based approaches, training-free methods aim to directly adapt vision-language models for open-vocabulary semantic segmentation without any training. Most training-free approaches focus on exploring to improve spatial coherence of image-level supervised CLIP. For instance, MaskCLIP [51] removes the self-attention at last layer, and directly employ value embeddings as output embeddings to perform pixel-level segmentation. Instead

of removing self-attention, SCLIP [34] and ClearCLIP [16] employ query-to-query or key-to-key attention map to replace original attention map at last layer. ProxyCLIP [15] first calculates the self-attention map of vision foundation model. CaR [33] adopts a recurrent framework to progressively enhance segmentation.

In addition, some researchers have explored to employ diffusion models for open-vocabulary semantic segmentation. For instance, ODISE [45] employs diffusion model to generate mask proposals, and generates the visual embeddings of masks for classification. OVDiff [13] generates support images of arbitrary categories using diffusion model, and extract the features of prototypes to segment inference images. DiffSegmenter [36] and iSeg [32] exploit self-attention and cross-attention maps from diffusion models for open-vocabulary segmentation.

In this paper, we explore to hierarchically improve spatial representation of CLIP for open-vocabulary semantic segmentation. CLIP demonstrates better zero-shot classification performance, while diffusion model is effective in capturing local details. Based on this, we first adopt CLIP to extract coarse segmentation map, and second employ diffusion model to refine the local details of segmentation map.

3. Methodology

Here, we first give some preliminaries of CLIP, Stable Diffusion, and attention mechanism. Afterwards, we introduce the motivation and our proposed method.

3.1. Preliminary

CLIP. CLIP [25] contains an image encoder and a text encoder. The image encoder comprises of a series of transformer blocks [10], where the input image is divided into patches and processed through these blocks. Each transformer block consists of a residual attention and a residual FFN. Initially, a class token is added to aggregate information from all image patches, forming a global representation of the image. Subsequently, each transformer block processes an input embeddings $F = [F_{cls}, F_1, \dots, F_{h \times w}]$, where F_{cls} represents the embeddings of class token, and others correspond to the embeddings of patch tokens. The output embeddings of class token is finally aligned with the embeddings generated by text encoder.

Stable Diffusion. Image diffusion model generates images starting from random Gaussian noise through a series of denoising steps. By training on large-scale dataset, the diffusion model Stable Diffusion [28] is able to generate high-quality images with rich details. It has been shown that, the features in Stable Diffusion are able to accurately capture local detail information. Therefore, we explore to use Stable Diffusion to improve local details of segmentation.

Attention mechanism. Both CLIP and Stable Diffusion leverage attention mechanism. Specifically, CLIP employs

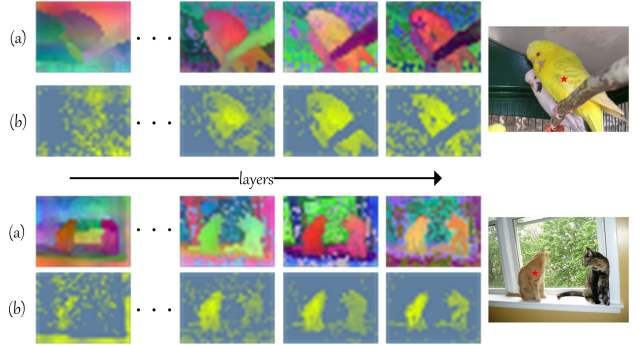


Figure 2. Visualization of path embeddings in CLIP. In (a), we visualize the embeddings into a 3D space and observe that the early embeddings exhibit good spatial coherence. In (b), we evaluate the cosine similarity between the embeddings of early layers at a specific point and the embeddings at last layer, revealing that the earlier and last embeddings share a similar embedding space.

the self-attention to model relationships between image patches. In contrast, Stable Diffusion incorporates both self-attention and cross-attention, where self-attention is used to extract spatial coherence within the image, and cross-attention allows the model to incorporate external conditioning information (*e.g.*, text description) to guide the image generation. The output of attention mechanism, whether in self-attention or cross-attention, is calculated by the query Q , key K and value V as follows

$$\text{Att}(Q, K, V) = A \times V, \quad (1)$$

the attention map A is given by

$$A = \text{Softmax}\left(\frac{QK^T}{\sqrt{d}}\right), \quad (2)$$

where d is the feature dimensionality of the key K . In self-attention, the query, key, and value all come from the same embeddings of image. In contrast, in cross-attention, the query comes from image, while the key and value come from text description.

3.2. Motivation

To adapt pre-trained CLIP for open-vocabulary segmentation, one straightforward approach is to discard the class token and use only the patch tokens to generate pixel-level similarity map with text embeddings. However, since CLIP is pre-trained on image-level classification task, this simple approach usually achieves poor segmentation due to weak spatial coherence of patch embeddings. To address this issue, some approaches [9, 34] primarily focus on modifying the last layer to improve spatial coherence. In contrast, we propose to hierarchically improve spatial representation for better segmentation from two aspects of observations.

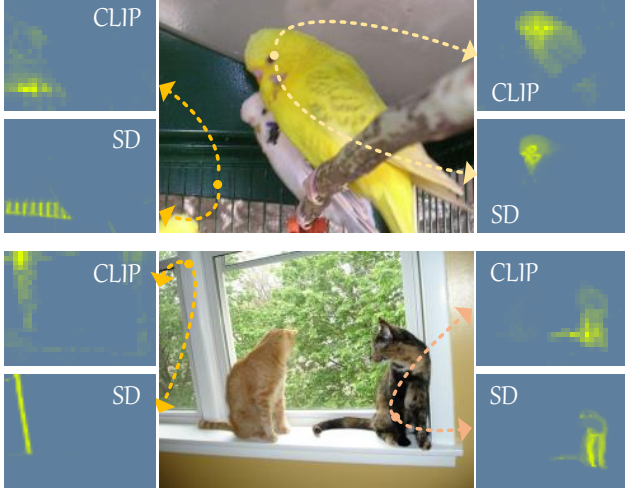


Figure 3. Visualization of self-attention maps between CLIP and Stable Diffusion (SD). We show the self-attention maps at selected points for both CLIP and SD. Compared to that of CLIP, we observe that the self-attention maps of SD focus more on capturing local details.

We observe that the embeddings at early layers are suitable for improving spatial coherence. First, as shown in Fig. 2(a), the patch embeddings at early layers retain consistent spatial information. Second, as in Fig. 2(b), early-layer embeddings share similarities with the embeddings at last layer. This similarity enables effective fusion of early- and late-layer information.

The pre-trained Stable Diffusion can generate high-quality images with rich details. As in Fig. 3, by visualizing the self-attention maps in both CLIP and Stable Diffusion, we observe that the attention maps of Stable Diffusion effectively capture local details. This contrasts with the attention maps in CLIP, which typically respond to broader semantic areas. This key observation suggests that we can integrate the fine spatial information from Stable Diffusion to improve coarse segmentation generated by CLIP.

3.3. Framework

Overview. Inspired by the motivation above, we propose a novel hierarchical approach for open-vocabulary semantic segmentation. Fig. 4 presents an overall architecture of our proposed method, named CLIPer. Our CLIPer consists of two complementary components. In first component, we leverage an early-layer fusion module to generate patch embeddings with better spatial coherence, and then generate coarse segmentation map according to the similarity between patch embeddings and text embeddings of text encoder. In second component, we perform fine-grained compensation using the attention maps of Stable Diffusion.

Early-layer fusion. This module aims to improve spatial coherence using the embeddings of early layers. Specifi-

cally, given an image, we first divide the image into patch embeddings $F^0 \in \mathbb{R}^{(hw+1) \times D}$, and then feed these embeddings to a series of transformer blocks. For the n -th transformer block, we generate the query Q^n , key K^n , and value V^n as

$$Q^n = \text{Proj}_q(\text{LN}(F^{n-1})), \quad (3)$$

$$K^n = \text{Proj}_k(\text{LN}(F^{n-1})), \quad (4)$$

$$V^n = \text{Proj}_v(\text{LN}(F^{n-1})). \quad (5)$$

Here, LN denotes layer normalization, and the projections Proj_q , Proj_k , and Proj_v respectively contain one learnable linear layer. With the query Q^n , key K^n , and value V^n , the output embeddings F^n of n -th transformer block are calculated by

$$\bar{F}^n = \text{Att}(Q^n, K^n, V^n) + F^{n-1}, \quad (6)$$

$$F^n = \text{FFN}(\text{LN}(\bar{F}^n)) + \bar{F}^n, \quad (7)$$

where FFN stands for a feed-forward network. The attention map of n -th transformer, which is generated in attention operation of Eq. 6, are denoted as A^n .

Similarly, we can generate the embeddings and attention maps of all transformer blocks up to the penultimate layer, denoted as two sets: $\mathcal{F} = \{F^i | i = 1, 2, \dots, N-1\}$ and $\mathcal{A} = \{A^i | i = 1, 2, \dots, N-1\}$. We first generate an averaged attention map as

$$A_{avg} = \frac{1}{N} \sum_{n=1}^{N-1} A^n. \quad (8)$$

Then, we replace the original self-attention map at last layer with the averaged attention map A_{avg} , and then feed all the embeddings to the last layer. Similar to ClearCLIP [16], we omit the feed-forward network and residual connections in the last transformer block, which can simplify the representation while aligning text embeddings better. As a result, we generate multiple output embeddings for different layers.

Lastly, we compute the cosine similarity between multiple output embeddings and text embeddings derived from the CLIP text encoder, and calculate the averaged similarity map. This averaged similarity map is used as the coarse segmentation by mapping each patch embedding to the candidate category embeddings.

Fine-grained compensation. The patch-level segmentation generated by CLIP remains relatively coarse, limiting segmentation accuracy. To better compensate local details of coarse map, we leverage the self-attention maps from Stable Diffusion, which we find to be particularly effective at capturing fine-grained local information. This locality-preserving characteristic is highly beneficial for refining the spatial details of patch-level segmentation, improving the ability to distinguish boundaries.

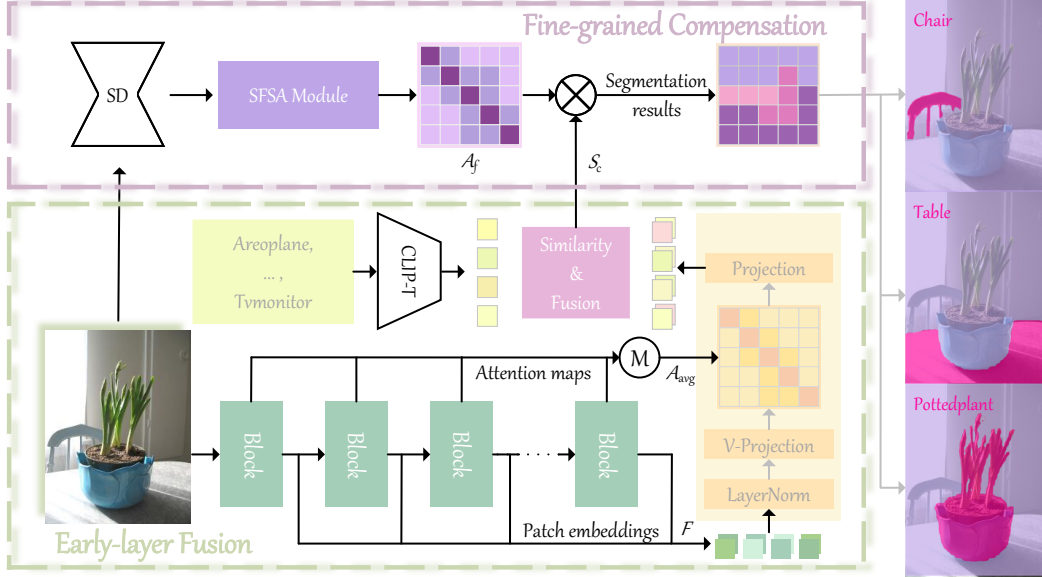


Figure 4. Overall architecture of our proposed method CLIPer. Our CLIPer contains two components: early-layer fusion and fine-grained compensation. In the early-layer fusion, we aggregate early-layer information of CLIP image encoder, including embeddings and attention maps, to improve spatial coherence of output embeddings, which are used to generate coarse segmentation map with text embeddings. The fine-grained compensation aims to employ self-attention maps of Stable Diffusion to refine local details of coarse segmentation map.

Specifically, we first feed the image along with an empty (null) textual prompt into Stable Diffusion, obtaining the corresponding multi-head self-attention maps at the highest spatial resolutions. We denote this attention maps as $A_m \in \mathbb{R}^{H \times L \times L}$, where H represents the number of attention heads, and L indicates the spatial size of feature maps in Stable Diffusion. Then, we fuse these attention maps A_m by matrix chain multiplication across the attention heads, which is formulated as

$$A_f = A_m[0] \times A_m[1] \times \cdots \times A_m[H-1], \quad (9)$$

where $A_m[i]$ means the i -th head self-attention map. Afterwards, we utilize the fused attention map A_f to refine the upscaled coarse segmentation map S_c as

$$S_f = A_f \times S_c. \quad (10)$$

Finally, we upscale S_f to the resolution of input image, yielding the fine-grained pixel-level segmentation map.

4. Experiment

Here we conduct experiments to demonstrate the effectiveness of our proposed method on various datasets.

4.1. Experimental Setups

Datasets. We evaluate CLIPer on seven datasets similar to most existing methods: (1) Considering the background category. We use PASCAL VOC (VOC) [11], PASCAL

Context (Context) [24], and COCO Object (Object) [3]; (2) Without considering the background category. We use PASCAL VOC (VOC20), PASCAL Context (Context59), COCO-Stuff (Stuff) [3], and ADE20K (ADE) [50]. For performance evaluation, we use the validation set from each dataset. In addition, for weakly supervised semantic segmentation, we evaluate the pseudo-mask generation performance on the training sets of VOC and COCO datasets.

Metrics. We use mean Intersection over Union (mIoU) to evaluate pixel-level segmentation accuracy. Further, we adopt mAP, F1 score, Precision (P), and Recall (R) to evaluate image-level classification performance.

Implementation details.

We implement our method on a single RTX 3090 with 24G memory. We employ ViT-B and ViT-L as the backbones, and uses Stable Diffusion V2.1 [28] for fine-grained compensation. In the Stable Diffusion, we extract the attention maps at time-step 45 in total of 50 steps. We set text prompts including category descriptions similar to SCLIP [34] and ProxyCLIP [15]. We resize all the input images to a shorter side of 336 pixels while maintaining the original aspect ratio, similar to ProxyCLIP [15]. Instead of using a sliding window strategy in [51], [34], [16] and [15], we directly feed the entire image into the CLIP image encoder, which is faster and simplifies the process.

4.2. Comparison With Other Methods

On mIoU. Table 1 compares our proposed method with some state-of-the-art methods on various datasets. Our pro-

Type	Method	Encoder	VOC	Context	Object	VOC20	Context59	Stuff	ADE
Training-based (weakly-supervised)	SegCLIP [23]	ViT-B/16	52.6	24.7	26.5	-	-	-	-
	ViewCo [27]	ViT-S/16	52.4	23.0	23.5	-	-	-	-
	OVSegmentor [44]	ViT-B/16	53.8	20.4	25.1	-	-	-	-
	CoCu [42]	ViT-S/16	51.4	23.6	22.7	-	-	22.1	12.3
	SAM-CLIP [18]	ViT-B/16	60.6	23.2	-	-	-	-	17.1
	GroupViT [43]	ViT-S/16	50.4	18.7	27.5	79.7	23.4	15.3	9.2
	TCL [5]	ViT-B/16	51.2	24.3	30.4	77.5	30.3	19.6	14.9
CLIP-DINOiser [37]	ViT-B/16	62.2	32.4	35.0	80.2	35.9	24.6	20.0	
Training-free	CLIP [25]	ViT-B/16	16.4	8.4	5.6	41.9	9.2	4.4	2.9
	CLIPSurgery [18]	ViT-B/16	-	29.3	-	-	-	21.9	-
	MaskCLIP [51]	ViT-B/16	38.8	23.6	20.6	74.9	26.4	16.4	9.8
	SCLIP [34]	ViT-B/16	59.1	30.4	30.5	80.4	34.2	22.4	16.1
	ClearCLIP [16]	ViT-B/16	51.8	32.6	33.0	80.9	35.9	23.9	16.7
	ProxyCLIP [15]	ViT-B/16	61.3	35.3	37.5	80.3	39.1	26.5	20.2
	CLIPer* (Ours)	ViT-B/16	60.1	34.8	36.0	84.0	38.5	25.3	19.8
	CLIPer (Ours)	ViT-B/16	65.9	37.6	39.0	85.2	41.7	27.5	21.4
	CLIP [25]	ViT-L/14	8.2	4.1	2.7	15.6	4.4	2.4	1.7
	MaskCLIP [51]	ViT-L/14	23.3	11.7	7.2	29.4	12.4	8.8	7.2
	SCLIP [34]	ViT-L/14	43.5	22.3	25.0	69.1	25.2	17.6	10.9
	ClearCLIP [16]	ViT-L/14	46.1	26.7	30.1	80.0	29.6	19.9	15.0
	CaR [33]	ViT-L/14	67.6	30.5	36.6	91.4	39.5	-	17.7
	ProxyCLIP [15]	ViT-L/14	60.6	34.5	39.2	83.2	37.7	25.6	22.6
	ProxyCLIP [15]	ViT-H/14	65.0	35.4	38.6	83.3	39.6	26.8	24.2
	CLIPer* (Ours)	ViT-L/14	61.2	34.3	39.6	88.2	39.8	25.8	21.8
	CLIPer (Ours)	ViT-L/14	69.8	38.0	43.3	90.0	43.6	28.7	24.4

Table 1. Comparison with existing open-vocabulary segmentation methods. * denotes our method without fine-grained compensation. Our method achieves state-of-the-art segmentation accuracy (mIoU) on all datasets, except VOC20 with the backbone ViT-L.

Method	Encoder	VOC				Context				Object			
		mAP	F1	P	R	mAP	F1	P	R	mAP	F1	P	R
CLIP [25]	ViT-L/14	90.2	75.3	79.7	71.3	59.8	54.2	55.1	53.2	66.3	53.7	57.9	50.0
MaskCLIP [51]	ViT-L/14	87.3	63.2	56.3	72.1	58.6	48.9	48.5	49.3	67.4	48.2	47.6	52.4
SCLIP [34]	ViT-L/14	92.7	74.5	81.0	69.1	63.2	57.7	57.6	57.7	71.4	55.4	64.5	48.6
ClearCLIP [16]	ViT-L/14	92.1	74.0	80.5	68.4	63.0	57.4	52.3	63.6	70.4	54.3	61.7	48.5
ProxyCLIP [15]	ViT-L/14	94.0	75.5	86.6	67.0	64.6	57.3	52.6	62.8	73.4	57.4	65.0	51.3
CLIPer (Ours)	ViT-L/14	94.6	86.0	86.7	85.3	68.9	63.3	63.4	64.3	77.9	62.3	69.7	56.3

Table 2. Comparison of image-level category classification capability with existing methods. We calculate classification scores of different categories by max-pooling the segmentation maps, and then calculates the results of mAP, F1, P, and R. Our method achieves the best results across all datasets, demonstrating its superior performance on category classification.

posed method almost achieves the best performance on all these datasets when using both ViT-B and ViT-L backbones. For instance, on VOC with the ViT-L backbone, SCLIP [34] has the mIoU score of 43.5%, ProxyCLIP [15] has the mIoU score of 60.6%, while our method achieves the mIoU score of 69.8%. Namely, our method outperforms SCLIP and ProxyCLIP by 26.3% and 9.2% on VOC. On ADE with the ViT-L backbone, ClearCLIP [16] and ProxyCLIP achieve the mIoU scores of 15.0% and 22.6%, while our method achieves the mIoU score of 24.4%. Namely, our method has the improvements of 9.4% and 1.8% on ADE.

On category classification and mask prediction. Open-vocabulary semantic segmentation can be viewed as two aspects: category classification and mask prediction. To deeply show the advantage of our proposed method on these two aspects, we provide more comparisons with other meth-

ods via two experiments. (i) We present image-level precision and recall comparison to show the advantages of identifying the categories within image. (ii) We compare the segmentation accuracy when giving image-level category labels, demonstrating the advantages of mask prediction. Weakly supervised semantic segmentation aims to train the model based on image-level category labels of training set. By comparing our method with weakly supervised approaches, we can demonstrate the benefits of our method in mask prediction.

In Table 2, we calculate image-level classification scores for all methods, and calculate the results using mAP, F1, P, and R. Our method achieves the best performance on all these metrics. It demonstrate that, our method can perform better on category classification, which is useful for open-vocabulary semantic segmentation.

Type	Method	VOC	COCO
Training-based	IRN [1]	66.5	42.4
	AdvCAM [17]	55.6	35.8
	MCTformer [46]	61.7	-
	ToCo [29]	72.2	-
	CLIMS [41]	56.6	-
Training-free	CLIP-ES [20]	70.8	39.7
	DiffSegmenter [36]	70.5	-
	T2M [38]	72.7	43.7
	iSeg [32]	75.2	45.5
	CLIPer (Ours)	76.9	47.3

Table 3. Comparison of pseudo-mask generation with weakly supervised semantic segmentation approaches. Both our method and these weakly supervised approaches predict corresponding pseudo masks according to given image-level category labels. Our CLIPer achieves the best results, showing that our method has better results on mask prediction.

Method	Encoder	Input size	Time(ms) ↓	mIoU ↑
ClearCLIP [16]	ViT-B/16	~ 448 × 624	22	51.8
ProxyCLIP [15]	ViT-B/16	~ 336 × 468	82	61.3
CLIPer* (Ours)	ViT-B/16	~ 336 × 468	14	60.1
CLIPer (Ours)	ViT-B/16	~ 336 × 468	158	65.9
ClearCLIP [16]	ViT-L/14	~ 448 × 624	68	46.1
ProxyCLIP [15]	ViT-L/14	~ 336 × 468	105	60.6
CLIPer* (Ours)	ViT-L/14	~ 336 × 468	47	61.2
CLIPer (Ours)	ViT-L/14	~ 336 × 468	192	69.8

Table 4. Comparison with other methods in terms of mIoU and inference time on VOC. * denotes the results obtained without fine-grained compensation. Our CLIPer* has the fastest speed, while Our CLIPer has the best performance.

Table 3 compares our method with some weakly supervised semantic segmentation approaches for pseudo mask generation, where the ground-truth image-level category labels are given. Compared to these weakly-supervised semantic segmentation approaches, our method achieves the best performance. For instance, our method outperforms CLIP-ES [20] and iSeg [32] by 6.1% and 1.7%. It demonstrates that, our method can improve mask prediction, and thus improving open-vocabulary semantic segmentation.

Inference time. Table 4 compares inference time and accuracy. Compared to ClearCLIP [16], our CLIPer* has faster speed and higher mIoU. Compared to ProxyCLIP [15], our CLIPer* has faster speed and comparable mIoU. Further, our CLIPer with fine-grained compensation significantly improvement the performance of CLIPer*.

Qualitative results. Fig. 5 presents some examples of qualitative comparison on VOC, Context, and Object. Our proposed method has more accurate segmentation maps and precise classification, compared to these methods [9, 15, 16]. For instance, our method has finer segmentation on bicycle and correct classification of person in second column, and accurate segmentation on sofa in fifth column.

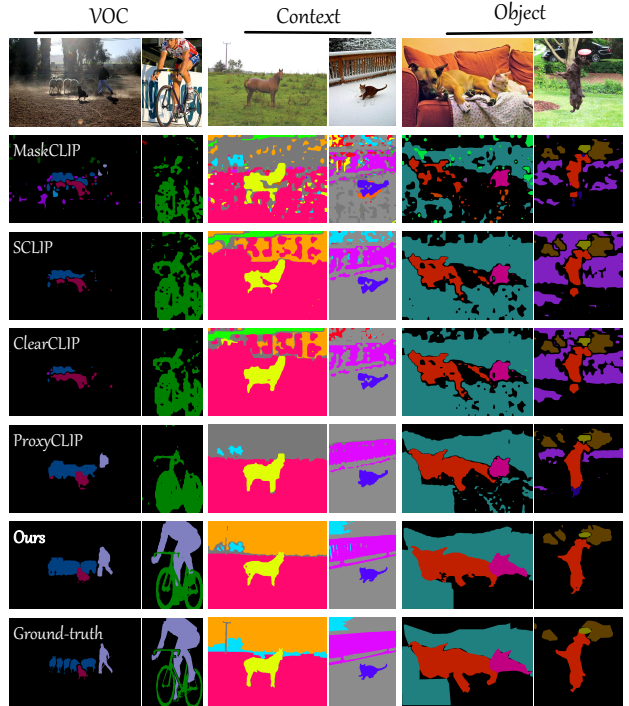


Figure 5. Qualitative comparison with existing methods. We show the segmentation results on three different datasets. Compared to these methods, our method has more accurate segmentation results which are closer to the ground-truths.

4.3. Ablation study

Impact of different modules. Table 5 presents the results of integrating difference modules into the baseline. The baseline replaces the original self-attention map at last layer with value-to-value attention map, and removes the feed-forward network (FFN) and residual connections. The baseline achieves the mIoU scores of 51.2%, 26.5%, and 32.3% on VOC, Context, and Object, respectively. When adding early-layer fusion (ELF) module, it has the mIoU scores of 61.2%, 34.3%, and 39.6% on VOC, Context, and Object, outperforming the baseline by 10.0%, 7.8%, 7.3%. When only using fine-grained compensation (FGC) module, it outperforms the baseline by 11.6%, 3.2%, 4.1%. When integrating the EFL and FGC modules together, it totally has the improvements of 18.6%, 11.5%, and 11.0% on three datasets, respectively. It can significantly demonstrate that, our proposed modules can improve open-vocabulary segmentation performance.

Effect of early-layer fusion. Table 6 compares our early-layer fusion with some self-self attention operations. Our early-layer fusion module fuses both the patch embeddings of early layers and the attention maps of early layers. In the top part, we compare our early-layer fused attention with these self-self attention operations, which all take the embeddings at last layer as input. Compared to these self-self

ELF	FGC	VOC	Context	Object
✗	✗	51.2	26.5	32.3
✓	✗	61.2	34.3	39.6
✗	✓	62.8	29.7	36.4
✓	✓	69.8	38.0	43.3

Table 5. Ablation study of different modules in our CLIPer. ELF represents early-layer fusion, and FGC represents fine-grained compensation. Our proposed modules can significantly improve the performance of the baseline.

Attention Type	Early-layer Embeddings	VOC	Context	Object
Query-query	✗	50.1	22.5	28.7
Key-key	✗	44.8	25.4	27.0
Value-value	✗	51.2	26.5	32.3
Identity matrix	✗	40.1	22.0	25.7
Early-layer attention	✗	58.6	33.1	38.4
Query-query	✓	55.7	26.9	32.0
Key-key	✓	53.2	29.5	33.1
Value-value	✓	54.8	29.4	34.4
Identity matrix	✓	43.3	24.8	27.8
Early-layer attention	✓	61.2	34.3	39.6

Table 6. Impact of different designs in our early-layer fusion. Our early-layer fusion contains fusing the embeddings and attention maps. In the top part, we compare our fused attention with some self-self attention operations. In the bottom part, we feed the early-layer embeddings to the attention map at last layer.

Type	VOC	Context	Object
Single	65.3	36.1	41.2
Mean	64.9	36.1	41.0
Multiplication	69.8	38.0	43.3

Table 7. Comparison of different strategies using the multi-head attention maps in Stable Diffusion. Single represents that, we evaluate each single head and report the best-performing head. Mean represents that, we average multi-head attention maps, and multiplication presents that, we perform matrix multiplication to fuse multi-head attention maps.

attention operations, our early-layer fused attention has the best performance. For instance, on VOC, Context, and Object, the query-query attention achieves the mIoU scores of 50.1%, 22.5%, and 28.7%, while our early-layer fused attention has the mIoU scores of 58.6%, 33.1%, and 38.4%. Namely, our early-layer fused attention outperforms query-query attention by 8.5%, 10.6%, and 9.7%, respectively.

In bottom part, we show the impact of feeding early-layer embeddings to last layer. When integrating early-layer embeddings into early-layer attention, it has the improvements of 2.6%, 1.2%, and 1.2% on VOC, Context, and Object, respectively. We observe that, using early-layer embeddings can also improve the performance of existing self-self attention operations. For instance, when combing it with value-value attention, it has the improvements of 3.6%, 2.9%, and 1.1% on VOC, Context, and Object, respectively.

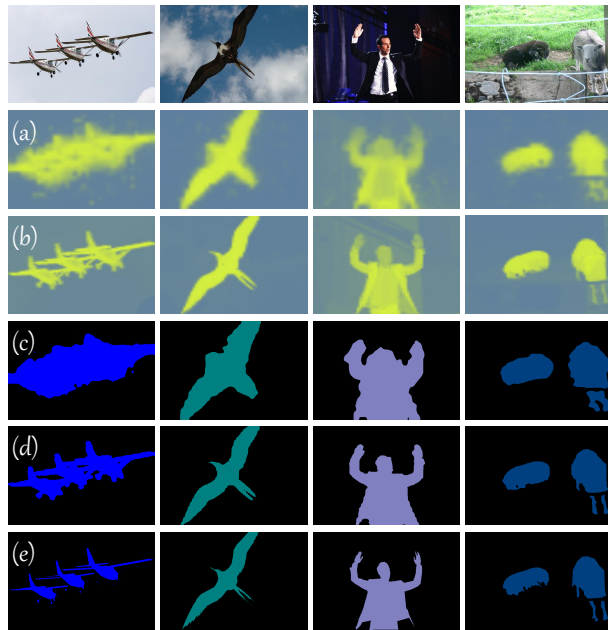


Figure 6. Visualization of fine-grained compensation. Given the input images in the top, we present the attention maps before and after fine-grained compensation in (a) and (b), show the binary segmentation maps in (c) and (d). We also present the ground-truth segmentation maps in (e).

Effect of fine-grained compensation. Table 7 presents different strategies to fuse the multi-head attention maps in Stable Diffusion for fine-grained compensation, including a single head (Single), averaging all heads (Mean), and combining all heads with matrix multiplication (multiplication). Compared to the baseline, all three strategies can improve the performance, demonstrating that the attention maps in Stable Diffusion can improve the CLIP-based segmentation. Among these strategies, matrix multiplication has the best performance, which is adopted as our final setting.

Fig. 6 shows some visualized examples before and after fine-grained compensation. Before fine-grained compensation, the attention maps in (b) provide coarse spatial structure information of objects. By using our fine-grained compensation, the attention maps in (c) are able to provide more accurate responses around object contour. As a result, compared to that in (d), using our fine-grained compensation has more accurate segmentation maps in (e). It demonstrates that, our fine-grained compensation can improve local details of coarse segmentation maps by early-layer fusion.

5. Conclusion

This paper presents CLIPer, a novel training-free method to hierarchically improve the spatial representation of CLIP for open-vocabulary semantic segmentation. To achieve this goal, we design two components, including early-layer

fusion and fine-grained compensation. The early-layer fusion aims to improve spatial coherence of output patch embeddings by using the early-layer information of patch embeddings and attention maps. The fine-grained compensation module employs the fine attention maps of diffusion model to further improve local details of segmentation maps. Our proposed method achieves the superior performance on various public segmentation datasets. We still observe that, our proposed method struggles from accurately segmenting the tiny objects. In the future, we will explore how to adapt the pre-trained model with high-resolution input for improving tiny object segmentation.

References

- [1] Jiwoon Ahn, Sunghyun Cho, and Suha Kwak. Weakly supervised learning of instance segmentation with inter-pixel relations. In *IEEE/CVF Conference on Computer Vision and Pattern Recognition*, pages 2209–2218, 2019. 7
- [2] Maxime Bucher, Tuan-Hung Vu, Matthieu Cord, and Patrick Pérez. Zero-shot semantic segmentation. In *Advances in Neural Information Processing Systems*, pages 468–479, 2019. 1
- [3] Holger Caesar, Jasper Uijlings, and Vittorio Ferrari. Coco-stuff: Thing and stuff classes in context. In *IEEE/CVF Conference on Computer Vision and Pattern Recognition*, pages 1209–1218, 2018. 5
- [4] Mathilde Caron, Hugo Touvron, Ishan Misra, Hervé Jégou, Julien Mairal, Piotr Bojanowski, and Armand Joulin. Emerging properties in self-supervised vision transformers. In *IEEE/CVF International Conference on Computer Vision*, pages 9650–19660, 2021. 2
- [5] Junbum Cha, Jonghwan Mun, and Byungseok Roh. Learning to generate text-grounded mask for open-world semantic segmentation from only image-text pairs. In *IEEE/CVF Conference on Computer Vision and Pattern Recognition*, pages 11165–11174, 2023. 2, 6
- [6] Bowen Cheng, Ishan Misra, Alexander G Schwing, Alexander Kirillov, and Rohit Girdhar. Masked-attention mask transformer for universal image segmentation. In *IEEE/CVF Conference on Computer Vision and Pattern Recognition*, pages 1290–1299, 2022. 2
- [7] Mehdi Cherti, Romain Beaumont, Ross Wightman, Mitchell Wortsman, Gabriel Ilharco, Cade Gordon, Christoph Schuhmann, Ludwig Schmidt, and Jenia Jitsev. Reproducible scaling laws for contrastive language-image learning. In *IEEE/CVF Conference on Computer Vision and Pattern Recognition*, pages 2818–2829, 2023. 2
- [8] Seokju Cho, Heeseong Shin, Sunghwan Hong, Seungjun An, Seungjun Lee, Anurag Arnab, Paul Hongsuck Seo, and Seungryong Kim. Cat-seg: Cost aggregation for open-vocabulary semantic segmentation. *arXiv preprint arXiv:2303.11797*, 2023. 1, 2
- [9] Zheng Ding, Jieke Wang, and Zhuowen Tu. Open-vocabulary panoptic segmentation with maskclip. *arXiv preprint arXiv:2208.08984*, 2022. 1, 2, 3, 7
- [10] Alexey Dosovitskiy, Lucas Beyer, Alexander Kolesnikov, Dirk Weissenborn, Xiaohua Zhai, Thomas Unterthiner, Mostafa Dehghani, Matthias Minderer, Georg Heigold, Sylvain Gelly, et al. An image is worth 16x16 words: Transformers for image recognition at scale. *arXiv preprint arXiv:2010.11929*, 2020. 3
- [11] Mark Everingham, Luc Van Gool, Christopher KI Williams, John Winn, and Andrew Zisserman. The pascal visual object classes (voc) challenge. *International Journal of Computer Vision*, 88:303–338, 2010. 5
- [12] Chao Jia, Yinfei Yang, Ye Xia, Yi-Ting Chen, Zarana Parekh, Hieu Pham, Quoc Le, Yun-Hsuan Sung, Zhen Li, and Tom Duerig. Scaling up visual and vision-language representation learning with noisy text supervision. In *International Conference on Machine Learning*, pages 4904–4916, 2021. 2
- [13] Laurynas Karazija, Iro Laina, Andrea Vedaldi, and Christian Rupprecht. Diffusion models for zero-shot open-vocabulary segmentation. In *European Conference on Computer Vision*, 2024. 3
- [14] Alexander Kirillov, Eric Mintun, Nikhila Ravi, Hanzi Mao, Chloe Rolland, Laura Gustafson, Tete Xiao, Spencer Whitehead, Alexander C Berg, Wan-Yen Lo, Piotr Dollar, and Ross Girshick. Segment anything. In *IEEE/CVF International Conference on Computer Vision*, pages 4015–4026, 2023. 2
- [15] Mengcheng Lan, Chaofeng Chen, Yiping Ke, Xinjiang Wang, Litong Feng, and Wayne Zhang. ProxyCLIP: Proxy attention improves clip for open-vocabulary segmentation. In *European Conference on Computer Vision*, 2024. 1, 2, 3, 5, 6, 7
- [16] Mengcheng Lan, Chaofeng Chen, Yiping Ke, Xinjiang Wang, Litong Feng, and Wayne Zhang. ClearCLIP: Decomposing clip representations for dense vision-language inference. In *European Conference on Computer Vision*, 2024. 1, 2, 3, 4, 5, 6, 7
- [17] Jungbeom Lee, Eunji Kim, and Sungroh Yoon. Anti-adversarially manipulated attributions for weakly and semi-supervised semantic segmentation. In *IEEE/CVF Conference on Computer Vision and Pattern Recognition*, pages 4071–4080, 2021. 7
- [18] Yi Li, Hualiang Wang, Yiqun Duan, Jiheng Zhang, and Xiaomeng Li. A closer look at the explainability of contrastive language-image pre-training. *arXiv preprint arXiv:2304.05653*, 2023. 6
- [19] Feng Liang, Bichen Wu, Xiaoliang Dai, Kunpeng Li, Yanan Zhao, Hang Zhang, Peizhao Zhang, Peter Vajda, and Diana Marculescu. Open-vocabulary semantic segmentation with mask-adapted clip. In *IEEE/CVF Conference on Computer Vision and Pattern Recognition*, pages 7061–7070, 2023. 2
- [20] Yuqi Lin, Minghao Chen, Wenxiao Wang, Boxi Wu, Ke Li, Binbin Lin, Haifeng Liu, and Xiaofei He. CLIP is also an efficient segmenter: A text-driven approach for weakly supervised semantic segmentation. In *IEEE/CVF Conference on Computer Vision and Pattern Recognition*, pages 15305–15314, 2023. 2, 7
- [21] Yuqi Lin, Minghao Chen, Kaipeng Zhang, Hengjia Li, Mingming Li, Zheng Yang, Dongqin Lv, Binbin Lin, Haifeng

- Liu, and Deng Cai. TagCLIP: A local-to-global framework to enhance open-vocabulary multi-label classification of clip without training. In *AAAI Conference on Artificial Intelligence*, pages 3513–3521, 2024. 2
- [22] Jonathan Long, Evan Shelhamer, and Trevor Darrell. Fully convolutional networks for semantic segmentation. In *IEEE/CVF Conference on Computer Vision and Pattern Recognition*, pages 431–440, 2015. 2
- [23] Huaishao Luo, Junwei Bao, Youzheng Wu, Xiaodong He, and Tianrui Li. SegCLIP: Patch aggregation with learnable centers for open-vocabulary semantic segmentation. In *International Conference on Machine Learning*, pages 23033–23044, 2023. 2, 6
- [24] Roozbeh Mottaghi, Xianjie Chen, Xiaobai Liu, Nam-Gyu Cho, Seong-Whan Lee, Sanja Fidler, Raquel Urtasun, and Alan Yuille. The role of context for object detection and semantic segmentation in the wild. In *IEEE Conference on Computer Vision and Pattern Recognition*, pages 891–898, 2014. 5
- [25] Alec Radford, Jong Wook Kim, Chris Hallacy, Aditya Ramesh, Gabriel Goh, Sandhini Agarwal, Girish Sastry, Amanda Askell, Pamela Mishkin, Jack Clark, Gretchen Krueger, and Ilya Sutskever. Learning transferable visual models from natural language supervision. In *International Conference on Machine Learning*, pages 8748–8763, 2021. 1, 2, 3, 6
- [26] Kanchana Ranasinghe, Brandon McKinzie, Sachin Ravi, Yinfei Yang, Alexander Toshev, and Jonathon Shlens. Perceptual grouping in contrastive vision-language models. In *IEEE/CVF International Conference on Computer Vision*, pages 5548–5561, 2023. 2
- [27] Pengzhen Ren, Changlin Li, Hang Xu, Yi Zhu, Guangrun Wang, Jianzhuang Liu, Xiaojun Chang, and Xiaodan Liang. ViewCo: Discovering text-supervised segmentation masks via multi-view semantic consistency. In *International Conference on Learning Representations*, 2023. 2, 6
- [28] Robin Rombach, Andreas Blattmann, Dominik Lorenz, Patrick Esser, and Björn Ommer. High-resolution image synthesis with latent diffusion models. In *IEEE/CVF Conference on Computer Vision and Pattern Recognition*, pages 10674–10685, 2022. 3, 5
- [29] Lixiang Ru, Heliang Zheng, Yibing Zhan, and Bo Du. Token contrast for weakly-supervised semantic segmentation. In *IEEE/CVF Conference on Computer Vision and Pattern Recognition*, pages 3093–3102, 2023. 7
- [30] Christoph Schuhmann, Romain Beaumont, Richard Vencu, Ross Wightman Cade Gordon, Mehdi Cherti, Theo Coombes, Aarush Katta, Clayton Mullis, Mitchell Wortsman, Patrick Schramowski, Srivatsa Kundurthy, Katherine Crowson, Ludwig Schmidt, Robert Kaczmarczyk, and Jenia Jitsev. Laion-5B: An open large-scale dataset for training next generation image-text models. In *International Conference on Neural Information Processing Systems*, pages 25278–25294, 2022. 2
- [31] Gyungin Shin, Weidi Xie, and Samuel Albanie. ReCo: Retrieve and co-segment for zero-shot transfer. In *International Conference on Neural Information Processing Systems*, pages 33754–33767, 2022. 2
- [32] Lin Sun, Jiale Cao, Jin Xie, Fahad Shahbaz Khan, and Yanwei Pang. iSeg: iseg: An iterative refinement-based framework for training-free segmentation. *arXiv preprint arXiv:2409.03209*, 2024. 3, 7
- [33] Shuyang Sun, Runjia Li, Philip Torr, Xiuye Gu, and Siyang Li. CLIP as RNN: Segment countless visual concepts without training endeavor. In *IEEE/CVF Conference on Computer Vision and Pattern Recognition*, pages 13171–13182, 2024. 3, 6
- [34] Feng Wang, Jieru Mei, and Alan Yuille. Sclip: Rethinking self-attention for dense vision-language inference. In *European Conference on Computer Vision*, pages 315–332, 2024. 1, 2, 3, 5, 6
- [35] Haoxiang Wang, Pavan Kumar Anasosalu Vasu, Fartash Faghri, Raviteja Vemulapalli, Mehrdad Farajtabar, Sachin Mehta, Mohammad Rastegari, Oncel Tuzel, and Hadi Pouransari. Sam-clip: Merging vision foundation models towards semantic and spatial understanding. In *IEEE/CVF Conference on Computer Vision and Pattern Recognition Workshops*, 2024. 2
- [36] Jinglong Wang, Xiawei Li, Jing Zhang, Qingyuan Xu, Qin Zhou, Qian Yu, Lu Sheng, and Dong Xu. Diffusion model is secretly a training-free open vocabulary semantic segmenter. *arXiv preprint arXiv:2309.02773*, 2023. 3, 7
- [37] Monika Wysoczańska, Oriane Siméoni, Michaël Ramamonjisoa, Andrei Bursuc, Tomasz Trzcziński, and Patrick Pérez. Clip-dinoiser: Teaching clip a few dino tricks for open-vocabulary semantic segmentation. *European Conference on Computer Vision*, pages 1–18, 2024. 6
- [38] Changming Xiao, Qi Yang, Zhou Feng, and Changshui Zhang. From text to mask: Localizing entities using the attention of text-to-image diffusion models. *arXiv preprint arXiv:2309.04109*, 2023. 7
- [39] Bin Xie, Jiale Cao, Jin Xie, Fahad Shahbaz Khan, and Yanwei Pang. Sed: A simple encoder-decoder for open-vocabulary semantic segmentation. In *IEEE/CVF Conference on Computer Vision and Pattern Recognition*, pages 3426–3436, 2024. 2
- [40] Enze Xie, Wenhai Wang, Zhiding Yu, Anima Anandkumar, Jose M. Alvarez, and Ping Luo. SegFormer: Simple and efficient design for semantic segmentation with transformers. In *International Conference on Neural Information Processing Systems*, pages 12077–12090, 2021. 2
- [41] Jinheng Xie, Xianxu Hou, Kai Ye, and Linlin Shen. Clims: Cross language image matching for weakly supervised semantic segmentation. In *IEEE/CVF Conference on Computer Vision and Pattern Recognition*, pages 4483–4492, 2022. 7
- [42] Yun Xing, Jian Kang, Aoran Xiao, Jiahao Nie, Shao Ling, and Shijian Lu. Rewrite caption semantics: Bridging semantic gaps for language-supervised semantic segmentation. In *Advances in Neural Information Processing Systems*, pages 68798–68809, 2023. 6
- [43] Jiarui Xu, Shalini De Mello, Sifei Liu, Wonmin Byeon, Thomas Breuel, Jan Kautz, and Xiaolong Wang. Groupvit: Semantic segmentation emerges from text supervision. In *IEEE/CVF Conference on Computer Vision and Pattern Recognition*, pages 18134–18144, 2022. 6

- [44] Jilan Xu, Junlin Hou, Yuejie Zhang, Rui Feng, Yi Wang, Yu Qiao, and Weidi Xie. Learning open-vocabulary semantic segmentation models from natural language supervision. In *IEEE/CVF Conference on Computer Vision and Pattern Recognition*, pages 2935–2944, 2023. [2](#), [6](#)
- [45] Jiarui Xu, Sifei Liu, Arash Vahdat, Wonmin Byeon, Xiaolong Wang, and Shalini De Mello. Open-vocabulary panoptic segmentation with text-to-image diffusion models. In *IEEE/CVF Conference on Computer Vision and Pattern Recognition*, pages 2955–2966, 2023. [2](#), [3](#)
- [46] Lian Xu, Wanli Ouyang, Mohammed Bennamoun, and Dan Xu. Multi-class token transformer for weakly supervised semantic segmentation. In *IEEE/CVF Conference on Computer Vision and Pattern Recognition*, pages 4310–4319, 2022. [7](#)
- [47] Mengde Xu, Zheng Zhang, Fangyun Wei, Han Hu, and Xiang Bai. Side adapter network for open-vocabulary semantic segmentation. In *IEEE/CVF Conference on Computer Vision and Pattern Recognition*, pages 2945–2954, 2023. [1](#), [2](#)
- [48] Qihang Yu, Ju He, Xueqing Deng, Xiaohui Shen, and Liang-Chieh Chen. Convolutions die hard: Open-vocabulary segmentation with single frozen convolutional clip. *arXiv preprint arXiv:2308.02487*, 2023. [1](#)
- [49] Hang Zhao, Xavier Puig, Bolei Zhou, Sanja Fidler, and Antonio Torralba. Open vocabulary scene parsing. In *IEEE/CVF International Conference on Computer Vision*, pages 2002–2010, 2017. [1](#)
- [50] Bolei Zhou, Hang Zhao, Xavier Puig, Tete Xiao, Sanja Fidler, Adela Barriuso, and Antonio Torralba. Semantic understanding of scenes through the ade20k dataset. *International Journal of Computer Vision*, 127:302–321, 2019. [5](#)
- [51] Chong Zhou, Chen Change Loy, and Bo Dai. Extract free dense labels from clip. In *European Conference on Computer Vision*, pages 696–712, 2022. [1](#), [2](#), [5](#), [6](#)